Colloid Polym Sci 280: 228–233 (2002)

ORIGINAL CONTRIBUTION

Tsuneo Okubo
Akira Tsuchida
Hideki Yoshimi
Kazumori Taguchi
Shigeharu Kiriyama

Rotational diffusion of tungstic acid colloids in microgravity as studied by aircraft experiments

Received: 22 February 2001
Accepted: 13 June 2001

T. Okubo (✉) · A. Tsuchida · H. Yoshimi
K. Taguchi · S. Kiriyama
Department of Applied Chemistry
Faculty of Engineering, Gifu University
Yanagido 1-1, Gifu 501-1193, Japan
e-mail: okubotsu@apchem.gifu-u.ac.jp
Fax: +81-58-2932628

Abstract Rotational relaxation times (τ) of anisotropic tungstic acid colloids (3.24 μm in major axis) in aqueous suspension are measured in microgravity ($0G$), normal gravity ($1G$) and at $2G$. The measurements at $0G$ and $2G$ are achieved by parabolic and circular flights, respectively. The limiting slopes of the relaxation curves in the plots of the transmitted light intensity against time are close to zero at $0G$ irrespective of the flow directions in the flow cell, whereas those at $1G$ and especially at $2G$ depend on the flow direction by the convection of the suspension and particle sedimentation. Experimental errors at the τ values at $0G$ are small compared with those at $1G$ and $2G$, which is ascribed to the lack of movement of impurities in the suspension such as quite small air bubbles, which cannot be recognized with the naked eye, and the convection of the suspension in microgravity. More reliable rotational relaxation times are obtained in microgravity; however, the relaxation times themselves are quite insensitive to gravity. The τ values observed are larger than those calculated from the particle size, which indicates the important contribution of the electrical double layers formed around the colloidal particles.

Keywords Rotational diffusion · Tungstic acid colloids · Microgravity experiments · Aircraft experiments · Electrical double layers

Introduction

A gravitational field is one of the important parameters for the physicochemical properties of colloidal suspensions [1–12]. It should be noted that the gravitational effect is significant for the translational diffusion of colloidal particles larger than 0.1 μm and heavier than 0.1 in the density difference of the particles against solvent ($\Delta\rho$). The Péclet number, Pe, which is the ratio of the time of sedimentation of a sphere in gravity against that of translational Brownian diffusion, is one of the convenient parameters needed to know the gravitational effect compared with the Brownian diffusion [13–16].

$$Pe = rS/D_t = \left(4\pi r^4 \Delta\rho g\right)/(3k_B T) \quad , \tag{1}$$

where r is the sphere radius, S and D_t the coefficients of sedimentation and translational diffusion, g the gravitational acceleration, k_B the Boltzmann constant and T the absolute temperature, respectively. For tungstic acid colloids the Pe is estimated to be about 230 when a sphere of 1.5 μm in radius and a specific gravity of 5.5 are assumed for simplicity for the calculation of a water suspension. Pe shows that the contribution of the sedimentation is much larger than that of diffusion. For the study of rotational relaxation of monodispersed colloids, tungstic acid colloids have many advantages, such as chemical stability, uniformity in their size, etc. However, the sedimentation of nonspherical particles, such as tungstic acid colloids in normal gravity, is complicated by the coupling of the rotational diffusion with the translational motion.

Flow birefringence, non-Newtonian flow, electric birefringence, fluorescence depolarization and dielectric dispersion are typical methods for the determination of the rotational diffusion coefficients (D_r) of anisotropically shaped colloids [17–21]. Okubo [22] proposed a stopped-flow technique as a new and convenient method for determining the rotational relaxation time (ranging from 1 ms to several seconds) of anisotropic colloidal particles, including ellipsoidal colloids of tungstic acid. The important role of the electrical double layers has been clarified for rotational diffusion.

In previous work [23, 24], the rotational relaxation times of tungstic acid colloids in aqueous media were determined in microgravity by free-fall experiments. Though, the duration of a microgravity was short (4.5 s), tungstic acid colloids are appropriate for the experiments, since their rotation should be complete within about 4 s for Perrin's equation; however, 4.5 s was not always long enough to obtain reliable slopes at either $1G$ or $0G$ [23, 24]. The main reason for this observation is due to the fact that the rotational diffusion is influenced by the interparticle interactions. Much more reliable data of the diffusion coefficients were obtained in microgravity, and the τ values in microgravity were quite the same as those in normal gravity. Furthermore, the very important role of the electrical double layers formed around the particles has been clarified. The accurate thickness of the layers has been evaluated in microgravity. The influences of additive sodium chloride and ethyl alcohol have been also studied.

In this work, the τ values were measured at $0G$ and $2G$ by parabolic and circular flights using an aircraft, respectively. The advantages of the aircraft experiments over the free-fall experiments are the long $0G$ duration (20–22 s) and the availability of the $2G$ experiments. The disadvantages of the aircraft experiments are the worse accuracy in the G values ($\pm 0.01G$) compared with the free-fall experiments ($\pm 0.001G$).

Experimental

Materials

Several samples of monodispersed ellipsoidal particles of tungstic acid were prepared and purified by the method of Furusawa and Hachisu [25]. HCl (25 ml, 1 N, Wako Pure Chemical Industries, Osaka) and Na_2WO_4 (50 ml, 7 wt% above 99% purity, Wako) were kept at 0–5 °C separately for more than 10 h before mixing. The two solutions were mixed homogeneously at once, and the mixture was left at room temperature for more than 10 h. A slightly yellowish gel of tungstic acid colloids was obtained. The gel was poured into 200 ml water, and then the suspension was stirred thoroughly. The suspension thus obtained was centrifuged (Kokusan, type H-9R, Tokyo) at 5,000–6,000 rpm for 480 s. The dispersion and the centrifuge processes were repeated five times, and the suspension (1.2 l) was incubated in a thermostated bath (changed from −1 to 30 °C, 2 °C for W55 particles) for more than 12 h. Then, monodispersed crystalloids appeared. The colloids thus obtained were further purified by repeated decantation.

Monodispersed tungstic acid colloids are thin ellipsoidal colloids whose major, middle and minor axes are represented by $2c$, $2b$ and $2a$, respectively. The standard deviation of the $2c$ and $2b$ values was within 6%. The lengths of the major axes ($2c$) of the colloids obtained (W1–W58) were determined using a metallurgical microscope (Olympus, PME3, Tokyo, ×400–1000). The cell used for the microscopic observation was the same as that described previously [22]. The size of the particles increased as the incubation temperature increased. Theoretical τ values were calculated from Perrin's equation [26] using the $2c$ values observed. The relationship between the values of b and c, $b = 0.41c$ was observed in our previous work [23, 24], and the values of the $2b$ length were evaluated using this equation. The minor axis ($2a$) was not determined experimentally in this work but was estimated from the data given in previous work [25] for electrophoresis measurements. The $2a$ values are estimated to be between 0.01 and 0.09 μm [27–29]. It should be noted that τ is very insensitive to the relatively small $2a$ value itself. $2c$, $2b$ and $2a$ of the W55 sample used in this work were estimated to be 3.24, 1.34 and 0.075 μm, respectively.

The water used for the preparation and purification of the sample suspensions was obtained from a Milli-Q water system (Millipore, Milli-RO Plus and Milli-Q Plus, Bedford, Mass.). The deionization of the suspension with ion-exchange resins was not performed in this work since the colloidal particles are slightly water soluble and ion-exchanged with hydroxide ions from the dissociation of water.

Measurements of rotational relaxation time

The rotational relaxation times (τ) were measured from the traces of the transmitted light intensity with time just after stopping the flow using the apparatus shown in Fig. 1. The instrument consists of a quartz flow cell (inner size: $1 \times 5 \times 40$ mm, Nakamura Glass Co., Kyoto) between two solenoid valves, Phamed tubes (inner diameter: 3.1 mm) and a peristaltic pump (Masterflex, 7524–10, Ill.). The pump circulates the colloidal suspension (about 40 ml) at a flow rate of 30 ml/min. Light from a light emitting diode (LED, Sansui, 12 V, 600–800 nm) passes through the cell and the transmitted light intensity is measured by a photodiode (Hamamatsu Photonics, S2281-01, Hamamatsu). The stability of the LED light intensity during $0G$ experiments has already been determined [23, 24]. The signal from a photodiode is led into a preamplifier (Hamamatsu, C2719) and into a homemade offset main amplifier. The total rise time of the instrument is less than 7 μs. The signals are finally recorded on an analogue-to-digital (A/D) converter (Contec, AD12-8 PM, Osaka, 10-μs interval) in a personal computer (Fujitsu, FMV, Tokyo). The signal is recorded from 5 s before the achievement of $0G$ (or $2G$) to 15 s after the recovery of $1G$. All the optical components around the cell are fixed tightly in a firm aluminum measurement box. Two flow cell systems are loaded on an aluminum bench, which can tilt 90° to change the flow direction in the measurement cell during the flights. Two sets of benches with two flow systems each are fitted on a rack for the aircraft; therefore, it is possible to measure four samples with different flow directions during a flight.

The flow directions of the sample suspension in the observation cell are shown in Fig. 2. The LED light always hits the cell center perpendicular to the largest plane. For the four flow directions (abbreviated as "up", "down", "back" and "side") the τ values were measured at $0G$, $1G$ and $2G$.

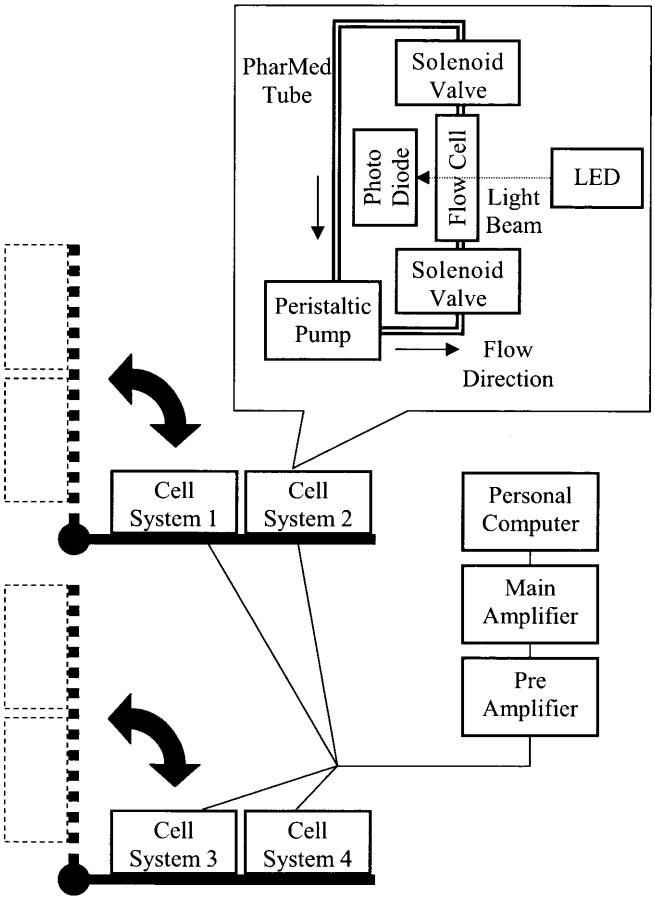

Fig. 1 Apparatus for the rotational relaxation time measurements

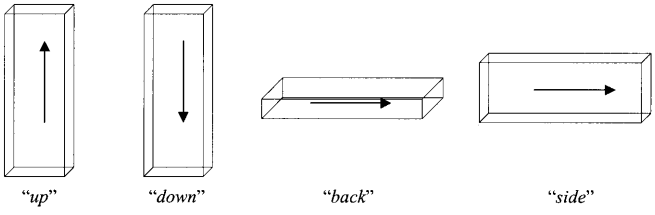

Fig. 2 Flow directions of the sample suspension

0*G* and 2*G* experiments were performed by parabolic and circular flights, respectively, using a Mitsubishi MU-300-type jet aircraft. The duration times of both 0*G* and 2*G* were 20–22 s. Errors in the values of 0*G* and 2*G* were about ± 0.01*G*. The temperatures of the cells were recorded by platinum sensors fitted on the cell boxes. Four types of measurements were made for each flight;

1. On the ground in a plane at 1*G* before flight.
2. During flight to the experimental area at 1*G*.
3. At 0G and 2*G* during the experimental flight.
4. On the ground in a plane at 1*G* after the flight.

Measurements 1 and 4 were made to obtain the reference data at 1*G* and to check the sedimentation of the particles during the flight. Measurement 2 was made to examine the influence of the vibration of the airplane.

Results and discussion

Relaxation traces in the transmitted light intensity

The major axes of ellipsoidal tungstic acid are oriented parallel to the flow direction in the cell during the continuous flow, which is due to the shearing forces arising from the velocity gradient. When the suspension flow is stopped, the colloidal particles revert to a random distribution by a free Brownian rotation. Translational diffusion is safely neglected in the stopped-flow method, since when the observation starts the flow of the solvent is stopped completely by the two solenoid valves located at both ends of the cell. The intensity of the transmitted light for the samples decreases and relaxes toward an equilibrium point after the flow is stopped.

The rotational diffusion constant, D_r, is evaluated from the τ values using Eq (2) [22].

$$D_r = 1/6\tau \tag{2}$$

The theoretical values of the D_r of ellipsoids are obtained using Perrin's equation, Eq (3) [26].

$$D_r = 3k_B T\left(a^2P + b^2Q\right)/16\pi\eta\left(a^2 + b^2\right) \ , \tag{3}$$

where k_B, T and η are the Boltzmann constant, the absolute temperature and the viscosity of the solvent, respectively. The constants P, Q and R are derived from Eqs. (4), (5) and (6).

$$P = \int_0^\infty \mathrm{d}s/\left(a^2 + s\right)\sqrt{(a^2 + s)(b^2 + s)(c^2 + s)} \ , \tag{4}$$

$$a^2P + b^2Q + c^2R = \int_0^\infty \mathrm{d}s/\sqrt{(a^2 + s)(b^2 + s)(c^2 + s)} \ , \tag{5}$$

$$P + Q + R = 2/abc, \quad a < b < c \ , \tag{6}$$

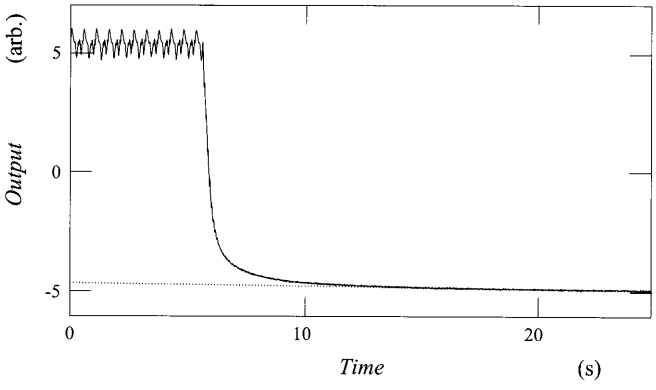

Fig. 3 Rotational relaxation curve of W55 particles at 27.0 °C. At 1*G*, 0.20 wt%, up flow. *Solid curve*: transmitted light intensity; *dotted line*: equilibrium linear fitting

where a, b and c denote the lengths of the minor, middle and major axes of the ellipsoidal colloids, respectively.

A typical example of the transmitted light intensity at 1G is shown in Fig. 3. The measurement was made in pure water for W55 particles in the upward flow direction at 1G on the ground. The ordinate designates the output voltage from a main amplifier. The large output means the large transmitted light intensity, and the values in the figure include the offset from the absolute output. $t = 0$ in the abscissa is the time when the A/D converter of the personal computer as a recorder was triggered. At around $t = 5.5$ s the pump was stopped. Circulation of the suspension was stopped completely within 0.1 s after stopping the pump, which was confirmed by the video camera observation. The large transmitted light intensity and its pulse caused by the pump are observed at about $t = 0$–5.5 s in the figure. After stopping the pump the output decreased. At around $t = 15$ s, the output converged to the limiting value, which indicates that almost random orientation of the colloidal particles is achieved. The dotted line in the figure shows the least-squares linear fitting between $t = 15$ and 22.5 s. It should be noted that the slope in this figure is negative, and the slope values depended strongly on the G values and the flow directions of the suspension in the measurement cell. After subtracting the values of the linear fitting line from those of the original curve, the decay part (in this case the fit was made for 4 to –4 in the ordinate) was least-squares fitted by an exponential function and a vertical shift. The rotational relaxation time is thus obtained from this exponential fitting.

A typical example of the traces for the transmitted light intensity at 0G is given in Fig. 4. All the experimental conditions except the G value and the suspension temperature were the same as those for Fig. 3. The differences in temperatures were finally compensated to 25 °C using the Perrin equation. Within 5 s after $t = 0$, a G sensor of the aircraft detected 0G, for example, a G value smaller than 0.1, and 0.5 s after the pump was stopped. Signal deviation from the horizontal line recorded at $t = 24$ s was caused by a slight flow induced in the cell when the parabolic flight was completed. In this figure the slope shown by the dotted line is close to zero.

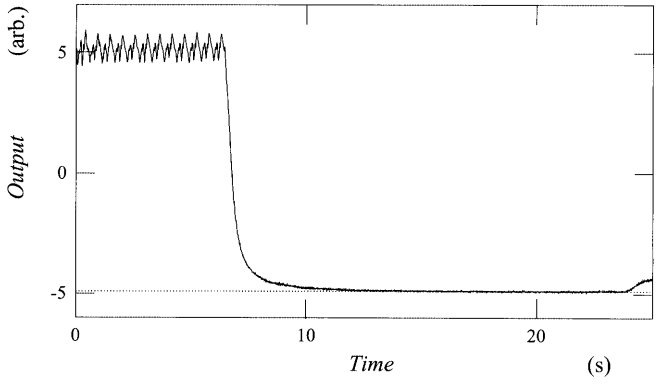

Fig. 4 Rotational relaxation curve of W55 particles at 27.2 °C. At 0G, 0.20 wt%, up flow. *Solid curve*: transmitted light intensity; *dotted line*: equilibrium linear fitting

The slopes in the relaxation traces

The limiting slopes at 0G, 1G and 2G are shown in Fig. 5 as a function of particle concentration. The slopes for suspension flow directions of up, down, back and side are represented by open circles, crosses, open triangles and open squares, respectively. The small and large marks indicate the measured and the average values, respectively.

The average slopes at 1G at the low particle concentrations were negative for the up, down and back directions, whereas those for side direction were positive. These results were the same as reported previously [23, 24]. The transmitted light measurements

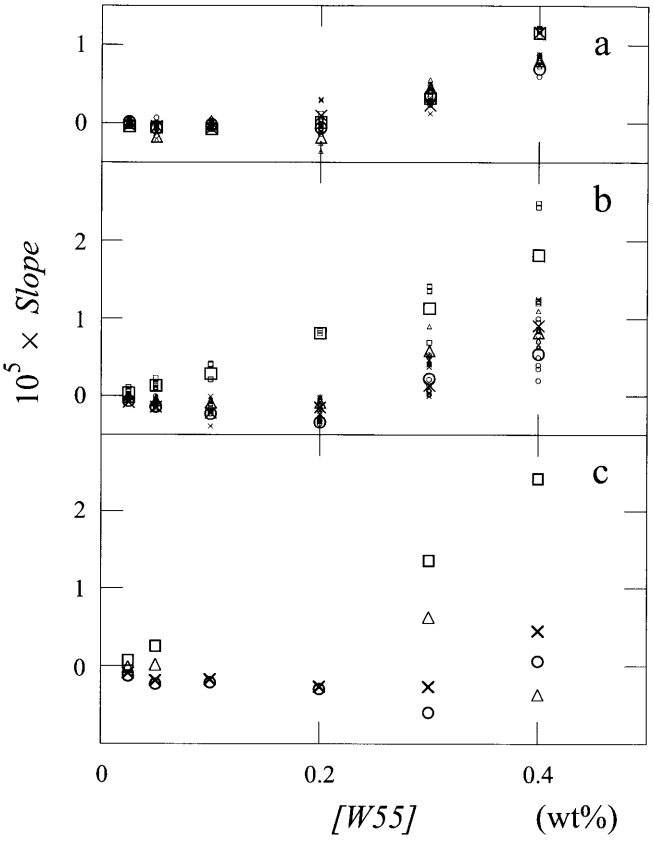

Fig. 5 Slopes of the final equilibrium lines in the rotational relaxation of W55 at **a** 0G, **b** 1G and **c** 2G. Suspension temperatures were compensated to 25 °C. Direction of flow: up (*circles*); down (*crosses*); back (*triangles*); side (*squares*). The *large marks* are the mean values of the experiments shown by the *small symbols*

were performed using the central 8-mm area within the total 40-mm length of the slender rectangular cell. If the number of colloidal particles in the observation area in the cell decreases owing to sedimentation by gravity, the transmitted light intensity should increase and then the slope becomes positive. Furthermore, the downward movement of the particles caused by gravity may result in particle orientation. For the up and down flow directions, this depletion zone of the colloidal particles by sedimentation does not occur in the central area in the observation position within 20–22 s for 0*G* and 2*G*. This depletion will not occur for the back flow direction. The reason for the negative slopes for these three directions is ascribed safely to the fact that the tail of the rotational relaxation still lasts in the range $t = 15$–22.5 s. On the other hand, for the side flow, the vertical height of the observation cell is so short (5 mm) that the depletion effects may occur within the observation time and then positive values in the slopes are observed.

The slopes at 0*G* for W55 ≤ 0.2 wt% were always close to zero irrespective of the flow direction (Fig. 5), whereas those at 1*G* shifted to negative ones for the up, down and back directions and to positive values for the side direction according to the increase in W55 concentration. It should be noted that the deviations at 2*G* of the slopes from zero are remarkably larger than those at 1*G* for W55 ≥ 0.2 wt%.

The slopes at 1*G* and 2*G* scattered greatly depending on the flow direction when compared with those at 0*G*. The main cause is the sedimentation of the particles in the observation cells as described earlier. We should further note that the convection of the suspension at 1*G* and 2*G* is one of the important causes of the large experimental error. Changes in the transmitted light intensity by the movement of very small impurities, such as dust and bubbles, which cannot be seen with the naked eye, are highly plausible at 1*G* and 2*G*. The values of the slope were very sensitive to the gravitational field, which is caused by the sedimentation of the particles keeping interparticle interactions such as mutual entanglement.

The rotational relaxation times

τ values at 0*G*, 1*G* and 2*G* are shown in Fig. 6 as a function of particle concentration. The samples are the same as those for Fig. 5. Clearly, the absolute values of τ were quite insensitive to gravity between 0*G* and 2*G*. However, the experimental errors in τ seem to decrease at 0*G* compared with those at 1*G* as is shown in the figure. Again, the lack of sedimentation and convection at 0*G* is the main cause for these observations. The τ values decreased sharply as the particle concentration increased, which is attributed to the thinning of the electrical double layers.

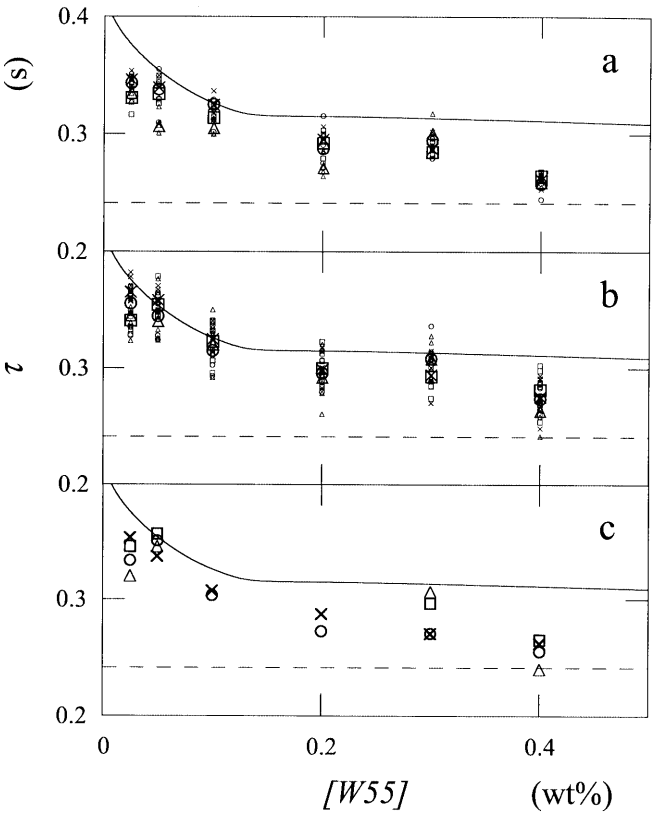

Fig. 6 Rotational relaxation times (τ) of W55 at **a** 0*G*, **b** 1*G* and **c** 2*G*. Suspension temperatures were compensated to 25 °C. Direction of flow: up (*circles*); down (*crosses*); back (*triangles*); side (*squares*). The *large marks* are the mean values of the experiments shown by the *small symbols*. *Solid curve*: calculated from the conductivity measurements using Perrin's equation; *broken line*: calculated at $D_l = 0$ nm

It should be noted here that the τ values observed were always larger than the values calculated using Eqs. (2), (3) (4), (5) and (6) [22]. Since the experiments were performed in the absence of foreign salt, the thickness of the electrical double layer, D_l, should be taken into account, i.e., the effective sizes including the thickness of the double layers for the minor, middle and major axes are given by $2a + 2D_l$, $2b + 2D_l$ and $2c + 2D_l$, respectively. Here, the thickness of the electrical double layer is given by

$$D_l = (4\pi Bn)^{-1/2} \quad , \tag{7}$$

where B is the Bjerrum length ($e^2/\varepsilon k_B T$, 0.719 nm at 25 °C) and n is the concentration of "free" (not bound to macroions) cations and anions in suspension. e and ε are the electronic charge and the dielectric constant of solvent, respectively. In the absence of foreign salt, n corresponds to the sum of the concentration of the free-state counterions (hydronium ions) and H^+ and OH^- ions from the dissociation of water.

The broken curves in the figure indicate the calculation of τ at $D_l = 0$ nm. The τ values calculated remain

constant irrespective of the particle concentration and are always smaller than the observed values. This difference demonstrates the important role of the electrical double layers formed around the colloidal particles, as has been discussed in previous work [23, 24]. The solid curves in the figure are the τ values calculated using Eqs. (2), (3), (4), (5) and (6) and the D_1 values estimated from the conductivity measurements of the sample suspensions. For example, the D_1 values were estimated to be 71, 80 and 132 nm from conductivities of 12.6, 10.1 and 3.69 μS/cm for 0.2, 0.1 and 0.01 wt% of W55 particles, respectively.

The solid curves locate close to the observations, but are slightly bigger than the observations, which is due to the fact that the double layers are so soft that they are deformed and even stripped away quite easily by the very weak shearing forces. The importance of the "electrostatic" intermacroion repulsion through the electrical double layers has been pointed out for the physicochemical properties of various colloidal suspensions, especially in salt-free systems hitherto [30–33].

Acknowledgements The authors thank the Space Forum Project (supported by the National Space Development Agency of Japan) for financial support. Diamond Air Service Co. (Aichi prefecture) is also acknowledged for carrying out the parabolic and circular flights. The Ministry of Education, Culture, Sports, Science and Technology, Japan, and the Japan Society for the Promotion of Science are also thanked for Grants-in-Aid for Scientific Research on Priority Area A (11167241) and for Scientific Research B (11450367), respectively. The quartz glass flow cells were made by Nakamura Glass Co. (Kyoto).

References

1. (1985, 1986) Microgravity polymers. NASA Conference Publication C-2392, Cleveland, Ohio
2. Schiffman RA (ed) (1988) Experimental methods for microgravity materials science research, vol 2. 2nd International Symposium. TMS CD-ROM Library, TMS
3. Schiffman RA (ed) (1992) Experimental methods for microgravity materials science research, vols 4–8. 4–8th International Symposia. TMS CD-ROM Library, TMS
4. Vanderhoff JW, El-Aasser MS, Micale FJ, et al (1986) PMSE Proc Am Chem Soc Div Polymer Mater Sci Eng 54:584
5. Briskman V, Kostarev K, Leontyev V, Levkovich M, Mashinsky A, Nechitailo G (1997) Proceedings of the 48th International Astronomy Congress, Turin, Italy. International Astronomy Federation, p 1–11
6. Zhu J, Li M, Rogers R, Meyer W, Ottewill RH, STS-73 Space Shuttle Crew, Russel WB, Chaikin PM (1997) Nature 387:883
7. Ishikawa M, Nakamura H, Kamei S, Okubo T, Morita TS, Kawasaki K, Kono Y (1996) J Jpn Soc Microgravity Appl 13:149–157
8. Ishikawa M, Nakamura H, Okubo T, Morita TS, Osada M, Tamaoki H, Kawasaki K, Koshikawa N, Nakamura Y, Nakakura T, Yoda S (1998) J Jpn Soc Microgravity Appl 15 Suppl II:168–172
9. Okubo T, Tsuchida A, Okuda T, Fujitsuna K, Ishikawa M, Morita T, Tada T (1999) Colloids Surf 153:515–524
10. Okubo T, Tsuchida A, Takahashi S, Taguchi K, Ishikawa M (2000) Colloid Polym Sci 278:202–210
11. Okubo T, Tsuchida A, Kobayashi K, Kuno A, Morita T, Fujishima M, Kohno Y (1999) Colloid Polym Sci 277:474–478
12. Tsuchida A, Taguchi K, Takyo E, Yoshimi H, Kiriyama S, Okubo T, Ishikawa M (2000) Colloid Polym Sci 278:872–877
13. Hunter RJ (1981) Zeta potential in colloid science. Principles and applications. Academic, London, p 117
14. Russel WB, Saville DA, Schowalter WR (1989) Colloidal dispersion. Cambridge University Press, Cambridge, p 394
15. van de Ven TGM (1989) Colloidal hydrodynamics. Academic, London, p 78
16. Hiemenz PC, Rajagopalan R (1977) Principles of colloid and surface chemistry, 3rd edn. Dekker, New York, p 176
17. Cohn EJ, Edsall JT (1943) Proteins, amino acids and peptides. Reinhold, New York
18. Weber G (1953) Adv Protein Chem 8:416
19. Jerrard HG (1959) Chem Rev 59:345
20. Frey M, Wahl P, Benoit H (1964) J Chim Phys 61:1005
21. Wierenga AM, Philipse AP, Reitsma EM (1997) Langmuir 13:6947
22. Okubo T (1987) J Am Chem Soc 109:1913
23. Okubo T, Tsuchida A, Yoshimi H, Maeda H (1999) Colloid Polym Sci 277: 601–606
24. Tsuchida A, Yoshimi H, Ohiwa K, Okubo T (2001) Colloid Polym Sci 279:427–433
25. Furusawa K, Hachisu S (1966) J Chem Soc Jpn 87:118
26. Perrin F (1934) J Phys Radium 5:497
27. Furusawa K, Hachisu S (1963) Sci Light 12:1
28. Furusawa K, Hachisu S (1963) Sci Light 12:15
29. Zocher VH, Jacobson K (1929) Kolloid Chem Beih 28:168
30. Hachisu S, Kobayashi Y, Kose A (1973) J Colloid Interface Sci 42:342
31. Pieranski P (1983) Contemp Phys 24:25
32. Okubo T (1988) Acc Chem Res 21:281
33. Okubo T (1993) Prog Polym Sci 18:481